LA-UR- 10-07762

Approved for public release; distribution is unlimited.

Title:	Combining Four Monte Carlo Estimators for Radiation Momentum Deposition
Author(s):	Joshua M. Hykes (North Carolina State University) and Todd J. Urbatsch (CCS-2, LANL)
Intended for:	International Conference on Mathematics and Computational Methods Applied to Nuclear Science and Engineering (M&C 2011), Rio de Janeiro, RJ, Brazil, Sponsored by Latin American Section (LAS)/American Nuclear Society (ANS), May 8-12, 2011

Los Alamos
NATIONAL LABORATORY
EST. 1943

Form 836 (7/06)

International Conference on Mathematics and Computational Methods Applied to Nuclear Science and Engineering (M&C 2011)
Rio de Janeiro, RJ, Brazil, May 8-12, 2011, on CD-ROM, Latin American Section (LAS) / American Nuclear Society (ANS)
ISBN 978-85-63688-00-2

COMBINING FOUR MONTE CARLO ESTIMATORS FOR RADIATION MOMENTUM DEPOSITION

Joshua M. Hykes
Department of Nuclear Engineering
North Carolina State University
Campus Box 7909, Raleigh, NC 27695
jmhykes@ncsu.edu

Todd J. Urbatsch
Los Alamos National Laboratory
PO Box 1663, MS D409, Los Alamos, NM 87545
tmonster@lanl.gov

ABSTRACT

Using four distinct Monte Carlo estimators for momentum deposition—analog, absorption, collision, and track-length estimators—we compute a combined estimator. In the wide range of problems tested, the combined estimator always has a figure of merit (FOM) equal to or better than the other estimators. In some instances the gain in FOM is only a few percent higher than the FOM of the best solo estimator, the track-length estimator, while in one instance it is better by a factor of 2.5. Over the majority of configurations, the combined estimator's FOM is 10–20% greater than any of the solo estimators' FOM. In addition, the numerical results show that the track-length estimator is the most important term in computing the combined estimator, followed far behind by the analog estimator. The absorption and collision estimators make negligible contributions.

Key Words: Momentum deposition, Monte Carlo

1. INTRODUCTION

Estimating the momentum deposited by radiation in the host medium can be an important piece of a hydrodynamics simulation. In the literature [2, 7], we have four different Monte Carlo estimators for estimating the momentum deposition at our disposal. As others have shown [1, 8], combining statistical estimators can be profitable. In most cases, the resulting estimate's variance is smaller than all of the constituent estimators' variances. It is only natural to apply this approach to the momentum deposition estimators.

The rest of the paper is organized as follows: First, we state the four estimators. Next, the equations for the combination are summarized with a short note on implementing them. Finally, a broad set of numerical results are presented. This paper describes the use of both analog-absorption tracking and implicit-absorption tracking (also known as implicit-capture tracking).

2. FOUR MOMENTUM DEPOSITION ESTIMATORS

The four momentum deposition estimators include one analog estimator and three non-analog estimators: the absorption, collision, and track-length estimators. These four estimators, described in detail by Hykes and Densmore [2], are briefly summarized here. The equations are directly from [2], using the same notation.

2.1 Analog Estimator

The standard method for estimating momentum deposition in Monte Carlo simulations is the analog estimator. The conceptually simplest of the four, this estimator tracks the momentum imparted at each particle interaction. See Urbatsch and Evans [7] for an example implementation.

To tally the momentum deposition in a cell with volume ΔV_c, sum over events

$$\vec{P}_{\text{dep},c} = \frac{1}{\Delta V_c} \sum_e \Delta \vec{P}_{\text{dep},c,e} \quad , \tag{1}$$

where $\Delta \vec{P}_{\text{dep},c,e}$ is the tally for a single event e in V_c, including all relevant events in the cell. For an absorption event, we tally

$$\Delta \vec{P}_{\text{dep},c,e} = \frac{\vec{\Omega}}{c} ew \quad . \tag{2}$$

where $\vec{\Omega}$ represents the particle direction at the time of a particular event, c is the speed of light, and ew is the energy-weight of the particle. In the case of implicit absorption, the tally is

$$\Delta \vec{P}_{\text{dep},c,e} = \frac{\vec{\Omega}}{c} (ew_{\text{old}} - ew_{\text{new}}) \quad . \tag{3}$$

For scattering, with $\vec{\Omega}_{\text{old}}$ as the incoming direction and $\vec{\Omega}_{\text{new}}$ as the outgoing direction, the momentum deposited at each scatter is

$$\Delta \vec{P}_{\text{dep},c,e} = \left(\frac{\vec{\Omega}_{\text{old}}}{c} - \frac{\vec{\Omega}_{\text{new}}}{c} \right) ew \quad . \tag{4}$$

For energy emitted by a radiation source in V_c, the tally is

$$\Delta \vec{P}_{\text{dep},c,e} = -\frac{\vec{\Omega}}{c} ew \quad . \tag{5}$$

The tally equations for the analog estimator are summarized in Table I.

2.2 Non-Analog Estimators

For the non-analog estimators, we estimate the integrals appearing in a volume-integrated first angular moment of the transport equation, as described in [2]. The contributions from isotropic sources sum to zero. The remaining integrals can be estimated by tallying absorptions, collisions, or particle tracks.

Absorption Estimator At each absorption event, one tallies

$$\Delta\vec{P}_{\text{dep},c,e} = \frac{\vec{\Omega}}{c}\frac{\sigma_{t,c} - \bar{\mu}_c\sigma_{s,c}}{\sigma_{a,c}} ew \quad ,$$

where $\sigma_{t,c}$, $\sigma_{s,c}$, and $\sigma_{a,c}$ are the total, scattering, and absorption opacities in V_c. The cosine of the mean scattering angle is $\bar{\mu}_c$. Treating implicit absorption as an absorption event, the tally in this case becomes

$$\Delta\vec{P}_{\text{dep},c,e} = \frac{\vec{\Omega}}{c}\frac{\sigma_{t,c} - \bar{\mu}_c\sigma_{s,c}}{\sigma_{a,c}}(ew_{\text{old}} - ew_{\text{new}}) \quad .$$

The tallies for the absorption estimator are summarized in Table II.

Collision Estimator Likewise for all collisions (both absorption and scatter), the collision estimator is

$$\Delta\vec{P}_{\text{dep},c,e} = \frac{\vec{\Omega}}{c}\frac{\sigma_{t,c} - \bar{\mu}_c\sigma_{s,c}}{\sigma_{t,c}} ew \quad ,$$

and at each implicit absorption

$$\Delta\vec{P}_{\text{dep},c,e} = \frac{\vec{\Omega}}{c}\frac{\sigma_{t,c} - \bar{\mu}_c\sigma_{s,c}}{\sigma_{t,c}}(ew_{\text{old}} - ew_{\text{new}}) \quad .$$

Note the only changes from the absorption estimator are the denominator from $\sigma_{a,c}$ to $\sigma_{t,c}$ and the inclusion of scattering events. The collision tallies are also stated in Table III.

Track-Length Estimator The track-length estimator estimates the integrals by tallying the total distance traveled by particles in the cell. With analog tracking (no implicit absorption), a particle's energy-weight is constant. In this case, for each path of distance l in V_c, we tally

$$\Delta\vec{P}_{\text{dep},c,e} = \frac{\vec{\Omega}}{c}(\sigma_{t,c} - \bar{\mu}_c\sigma_{s,c}) ew\, l \quad .$$

For implicit absorption, the proper tally is

$$\Delta\vec{P}_{\text{dep},c,e} = \frac{\vec{\Omega}}{c}\frac{\sigma_{t,c} - \bar{\mu}_c\sigma_{s,c}}{\sigma_{a,c}}(ew_{\text{old}} - ew_{\text{new}}) \quad .$$

The tallies for the track-length estimator are summarized in Table IV. With implicit absorption, the absorption and track-length estimators are nearly equivalent. (They not are identical because implicit-absorption tracking switches to analog-absorption tracking when a particle falls beneath the critical energy-weight.)

Table I: Tallies for the analog estimator [2]

Event	$\Delta\vec{P}_{\text{dep},c,e}$
Absorption	$\frac{\vec{\Omega}}{c} ew$
Implicit absorption	$\frac{\vec{\Omega}}{c}(ew_{\text{old}} - ew_{\text{new}})$
Scatter	$\left(\frac{\vec{\Omega}_{\text{old}}}{c} - \frac{\vec{\Omega}_{\text{new}}}{c}\right) ew$
Source	$-\frac{\vec{\Omega}}{c} ew$

Table II: Tallies for the absorption estimator [2]

Event	$\Delta\vec{P}_{\text{dep},c,e}$
Absorption	$\frac{\vec{\Omega}}{c}\frac{\sigma_{t,c} - \bar{\mu}_c\sigma_{s,c}}{\sigma_{a,c}} ew$
Implicit absorption	$\frac{\vec{\Omega}}{c}\frac{\sigma_{t,c} - \bar{\mu}_c\sigma_{s,c}}{\sigma_{a,c}}(ew_{\text{old}} - ew_{\text{new}})$

Table III: Tallies for the collision estimator [2]

Event	$\Delta\vec{P}_{\text{dep},c,e}$
Collision	$\frac{\vec{\Omega}}{c}\frac{\sigma_{t,c} - \bar{\mu}_c\sigma_{s,c}}{\sigma_{t,c}} ew$
Implicit absorption	$\frac{\vec{\Omega}}{c}\frac{\sigma_{t,c} - \bar{\mu}_c\sigma_{s,c}}{\sigma_{t,c}}(ew_{\text{old}} - ew_{\text{new}})$

Table IV: Tallies for the track-length estimator [2]

Tracking	$\Delta\vec{P}_{\text{dep},c,e}$
Analog	$\frac{\vec{\Omega}}{c}(\sigma_{t,c} - \bar{\mu}_c\sigma_{s,c}) ew\, l$
Implicit absorption	$\frac{\vec{\Omega}}{c}\frac{\sigma_{t,c} - \bar{\mu}_c\sigma_{s,c}}{\sigma_{a,c}}(ew_{\text{old}} - ew_{\text{new}})$

3. COMBINING CORRELATED ESTIMATES WITH UNEQUAL VARIANCES

The problem of combining estimates is common. For independent estimates with unequal variances, the combined estimate is a linear sum of the estimates with the weights determined by the estimates' variances. In the case at hand, the estimates can not be assumed independent, so we must estimate and use the full covariance matrix.

Halperin rigorously addressed this problem [1]. Urbatsch and others in [8, 9] provide some helpful comments to understand Halperin's rather terse paper, as well as demonstrating the method for two and three k_{eff} estimators. Using Halperin's notation, we have k estimates, each of which was computed from n samples. All of the sample data can be placed in a set $\{x_{1,1},\ldots,x_{1,n};x_{2,1},\ldots,x_{2,n};\cdots;x_{k,1},\ldots,x_{k,n}\}$, where the first index goes with k and the second with n. The means of the k subsets, computed as $\bar{x}_i = \sum_{p=1}^{n} x_{i,p}/n$, can be placed in a vector $\bar{\mathbf{x}} = [\bar{x}_1,\ldots,\bar{x}_k]^T$. In the present paper, n is the number of particle histories and k is the number of estimators. The true estimators' variances and covariances are unknown, but we approximate them with the sample variances and covariances. The sample covariance matrix $\hat{\boldsymbol{\Sigma}}$ approximates the true covariance matrix $\boldsymbol{\Sigma}$. Both matrices have size $k \times k$. The (i, j) element of the sample covariance matrix is computed as

$$[\hat{\boldsymbol{\Sigma}}]_{i,j} = \frac{1}{n-1}\sum_{p=1}^{n}(x_{i,p}-\bar{x}_i)(x_{j,p}-\bar{x}_j) \quad .$$

Eventually Halperin comes to the approximation of the true mean μ by an approximate combined estimate,

$$\hat{\mu} = \frac{\mathbf{e}^T\hat{\boldsymbol{\Sigma}}^{-1}\bar{\mathbf{x}}}{\mathbf{e}^T\hat{\boldsymbol{\Sigma}}^{-1}\mathbf{e}} \quad , \tag{6}$$

where $\mathbf{e}$ is the k-vector $[1,\ldots,1]^T$. Furthermore, the variance of $\hat{\mu}$ can be computed as

$$\sigma^2_{\hat{\mu}} = \frac{n-1}{n-r}\frac{1}{\mathbf{e}^T\hat{\boldsymbol{\Sigma}}^{-1}\mathbf{e}}\left(\frac{1}{n}+\mathbf{d}^T\mathbf{S}_d^{-1}\mathbf{d}\right) \quad , \tag{7}$$

where $\mathbf{S}_d$ is the $(k-1)\times(k-1)$ submatrix of $(n-1)\hat{\boldsymbol{\Sigma}}$ which excludes the first row and column of $(n-1)\hat{\boldsymbol{\Sigma}}$. The $(k-1)$-vector $\mathbf{d}$ is $[\bar{x}_1-\bar{x}_2,\bar{x}_1-\bar{x}_3,\ldots,\bar{x}_1-\bar{x}_k]^T$. The numerical rank of $\hat{\boldsymbol{\Sigma}}$ is r (see §3.1). The $(n-1)/(n-r)$ factor makes the estimator unbiased, since we have already used r degrees of freedom to compute the means. For large n, this term is nearly equal to one.

See Halperin's paper [1] and the report by Urbatsch and others [8] for the derivations of these equations.

3.1 Implementation Issues

Urbatsch and his coauthors [8] solved Eqns. (6–7) symbolically. For the combination of two variables, the final expressions were reasonably compact, but for three variables, the expressions spanned several lines. Partly to avoid the algebraic complexity, we have implemented the combination equations using numerical linear algebra, with the two main tasks being the inversion of $\hat{\boldsymbol{\Sigma}}$ and $\mathbf{S}_d$. Since these matrices have size four and three, respectively, the computational costs are low, and direct methods are an obvious choice.

The main difficulty in the numerical approach occurs when two estimators are highly correlated or identical. For instance, using implicit-absorption tracking, the absorption and track-length estimators are almost

identical. The rank of the covariance matrix is then only three instead of four, and the matrix is singular and non-invertible. Thus, using an LU or related Gaussian elimination method to compute the solution to the linear system is untenable.

We desire a simple and robust method which automatically identifies and corrects for high correlations and resulting rank deficiency. We choose to implement an algorithm based on the rank-revealing singular value decomposition (SVD), $\hat{\mathbf{\Sigma}} = \mathbf{USV}^T$, where $\mathbf{S}$ is a diagonal matrix comprising the singular values $\sigma_1 \geq \sigma_2 \geq \cdots \geq \sigma_n$, $\mathbf{U}$ and $\mathbf{V}$ are unitary matrices containing the right and left singular vectors $\mathbf{u}_i$ and $\mathbf{v}_i$ of $\hat{\mathbf{\Sigma}}$, and $\hat{\mathbf{\Sigma}}, \mathbf{U}, \mathbf{S}, \mathbf{V} \in \mathbb{R}^{n \times n}$. See the text by Meyer for more details [6]. For a matrix of rank r, the pseudoinverse of $\hat{\mathbf{\Sigma}}$ is defined as [6]

$$\hat{\mathbf{\Sigma}}^{\dagger} = \sum_{i=1}^{r} \frac{\mathbf{v}_i \mathbf{u}_i^T}{\sigma_i} \quad .$$

The magnitudes of the singular values are the key to determining the rank, or more appropriately, the numerical rank. The rank r matrix has r "large" singular values and $n - r$ "small" singular values. A gap of several orders of magnitude usually separates the large and small singular values. In the present implementation, r was chosen to satisfy the test $\sigma_i/\sigma_1 > \delta$ for $i = 1, \ldots, r$, where $\delta = \epsilon_m n$. Here ϵ_m is the machine epsilon. This is the tolerance used by the `pinv` function in Matlab [5], but it can be tuned if needed. This method of ignoring the contributions from the smallest singular values is commonly referred to as truncated SVD.

The pseudoinverse correctly deals with a number of cases in which the covariance matrix was singular or nearly singular. This includes when two estimators are identical, as are the absorption and collision estimators in purely-absorbing media. The method also successfully handles nearly identical estimators, such as absorption and track-length estimators with implicit-absorption tracking. In our test problems the method proved to be robust.

4. NUMERICAL RESULTS

We characterize the behavior of the combined estimator using the same set of one-dimensional tests from [2]. The radiative transfer equation simplifies to

$$\mu \frac{\partial I}{\partial z} + \sigma_t I = \frac{\sigma_s}{2} \int_{-1}^{1} I(z, \mu')\, d\mu' + \frac{Q}{2} \quad , \tag{8}$$

where we assume isotropic scattering and slab geometry. For simplicity, we treat the dimensionless problem. The domain of the independent variables is $z \in [0, 1]$ in space and $\mu \in [-1, 1]$ in angle. The material is spatially homogeneous. We impose an isotropic incident intensity on the left boundary,

$$I(0, \mu) = \frac{\phi}{2} \quad , \quad 0 < \mu \leq 1 \quad , \tag{9}$$

with ϕ a constant, and a vacuum on the right boundary,

$$I(1, \mu) = 0 \quad , \quad -1 \leq \mu < 0 \quad . \tag{10}$$

For simplicity, we set the speed of light equal to unity.

To explore a diverse set of material properties, we express the total opacity, total scattering opacity, and radiation source in Eq. (8) as follows:

$$\sigma_t = \frac{1}{\epsilon} \quad ; \tag{11}$$

$$\sigma_s = \frac{1}{\epsilon} - \epsilon \quad ; \tag{12}$$

$$Q = \epsilon q \quad . \tag{13}$$

In Eq. (13), q is another constant, and $\epsilon \in (0, 1]$ is a scaling parameter. For $\epsilon = 1$, the scattering opacity vanishes, creating a purely absorbing problem. As $\epsilon \to 0$, the material becomes highly scattering, and the problem is in the asymptotic diffusion limit [3].

The following numerical demonstrations fall into two groups. The first group lacks a radiation source ($q = Q = 0$), but an isotropic incident intensity is specified as the left boundary condition. To have the rate of energy entering the slab equal one,

$$\int_0^1 \mu I(0, \mu)\, d\mu = \frac{\phi}{4} = 1 \quad . \tag{14}$$

we set $\phi = 4$ in Eq. (9).

For the second group, both the right and left boundary conditions are vacuum ($\phi = 0$), but we insert a radiation source by letting $q = 1$.

For these two groups of problems, we have constructed test problems of the two types described above with various values of ϵ and have calculated momentum deposition in each problem using all five estimators (the four solo estimators and the one combined estimator) for both analog tracking and implicit absorption. We collected tallies by dividing the problem domain into ten equally-sized spatial cells. Each simulation consisted of 10^7 particle histories. The performance of each estimator is measured by the figure of merit (FOM) [4],

$$\text{FOM} = \frac{\hat{x}^2}{\sigma^2(\hat{x})T} \quad . \tag{15}$$

Here, $\hat{x}$ is the estimate of momentum deposition averaged over all particle histories, $\sigma(\hat{x})$ is the corresponding standard deviation, and T is the total computer time required to complete all particle histories. Because lower standard deviations and shorter computer times are favorable, we associate a higher FOM with better performance. We can also view the FOM in this case as a measure of the standard deviation, because the various estimators do not affect particle histories (unlike many variance-reduction techniques), and thus computer times do not differ significantly between estimators for a specific problem and tracking method.

For each test, the FOM for each of the five estimators was computed for each spatial cell. Next, the absorption, collision, track-length, and combined estimators' FOM were normalized to the analog FOM, again for each cell. To be concise, only the mean, maximum, and minimum normalized FOM over all spatial cells are plotted, allowing the effect of ϵ to be clear.

In addition to the normalized FOM plots for the four estimators, we include, for qualitative purposes, an example of the estimates and standard deviations with increasing histories. Also, since the track-length estimator is the best solo estimator, one figure makes a head-to-head comparison of the combined to track-length estimator. Finally, the weighting factors used to compute the combined estimator are presented. However, the solutions to the problems are not presented here; the interested reader can find them in [2].

4.1 Incident-Intensity Problems

Analog-absorption tracking In this section, we present the results from the incident intensity problem using analog-absorption tracking. Before moving to the purely quantitative FOM results, we provide a visual

demonstration of the benefits of the combined estimator in Figure 1. This is the momentum deposited in the far left tally cell with $\epsilon = 1/2$. The track-length and combined estimators are clearly superior to the other three estimators. While not drastic, the advantage of the combined over the track-length estimator is evident. With the following figures, we use the FOM to quantify this gain. Figure 2 demonstrates the performance of the combined estimator in relation to the others. The top line in each shaded area represents the maximum normalized FOM over the slab width, while the bottom line represents the minimum FOM ratio over the slab. The darker line in the interior represents the mean.

Implicit-absorption tracking Figure 3 illustrates the performance of the combined estimator for an incident intensity with implicit-absorption tracking. The absorption and track-length estimators are nearly identical, so their normalized FOM is only plotted once. Notice that for purely-absorbing media, when $\epsilon = 1$, the performance of all the estimators is the same, or nearly so. In this case, all the estimators are identical or highly correlated, and the covariance matrix has a numerical rank of one. The truncated SVD solution gives the answer we expect: the combination of four identical estimates is the same estimate.

4.2 Radiation-Source Problems

Analog-absorption tracking Figure 4 shows the performance of the combined estimator in relation to the others for the radiation-source problem using analog-absorption tracking.

Implicit-absorption tracking Figure 5 presents the performance of the combined estimator for a radiation-source with implicit-absorption tracking. As for the incident intensity with implicit-absorption tracking, the absorption and track-length estimators are nearly identical, so their normalized FOM is only plotted once.

4.3 Combined and Track-length Estimator Comparison

Since the track-length and combined estimators are often an order-of-magnitude or more better than the other solo estimators, Figures 2–5 make it difficult to directly compare the two best estimators. Figure 6 ameliorates this issue by plotting the ratio of the combined FOM to the track-length FOM on a linear scale. The ten spatial cells are again collapsed into the minimum, maximum, and mean at each ϵ, as above. The combined estimator FOM is always greater than or equal to the track-length estimator FOM. The mean ratios are primarily in the range 1.1–1.2. The largest ratio achieved is 2.5.

4.4 Watching our Weights

The combined estimator is computed by a weighted sum of the four solo estimators. The components of the weight vector $\mathbf{w} = (\mathbf{e}^T\hat{\boldsymbol{\Sigma}}^{-1}\mathbf{e})^{-1}\mathbf{e}^T\hat{\boldsymbol{\Sigma}}^{-1}$ are plotted in Figure 7 for each of the four cases. For the implicit-absorption cases, where the absorption and track-length estimators are nearly identical, we only display the sum of the weights instead of plotting the two separately. The four figures are remarkable for their similarity. The track-length weight is greater than 0.8, and the analog weight is less than 0.2. The weights for the other two estimators are negligible (with the exception of the absorption estimator for implicit-absorption tracking).

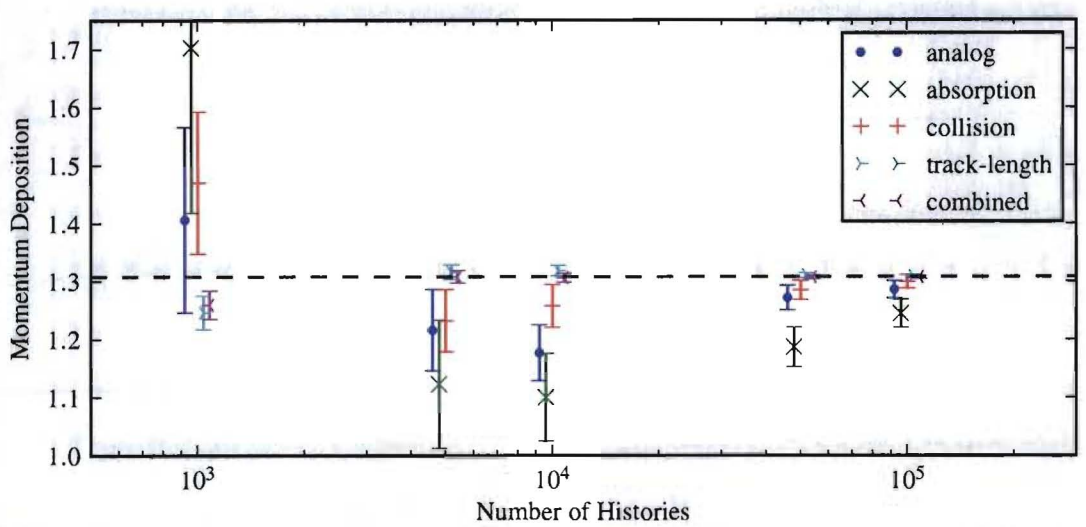

(a) Qualitative comparison of the performance of the momentum deposition estimators. The error bars represent one standard deviation. The dotted black line represents the converged solution with $5 \cdot 10^6$ histories. The horizontal spacing between points in each clump is added only for ease of viewing.

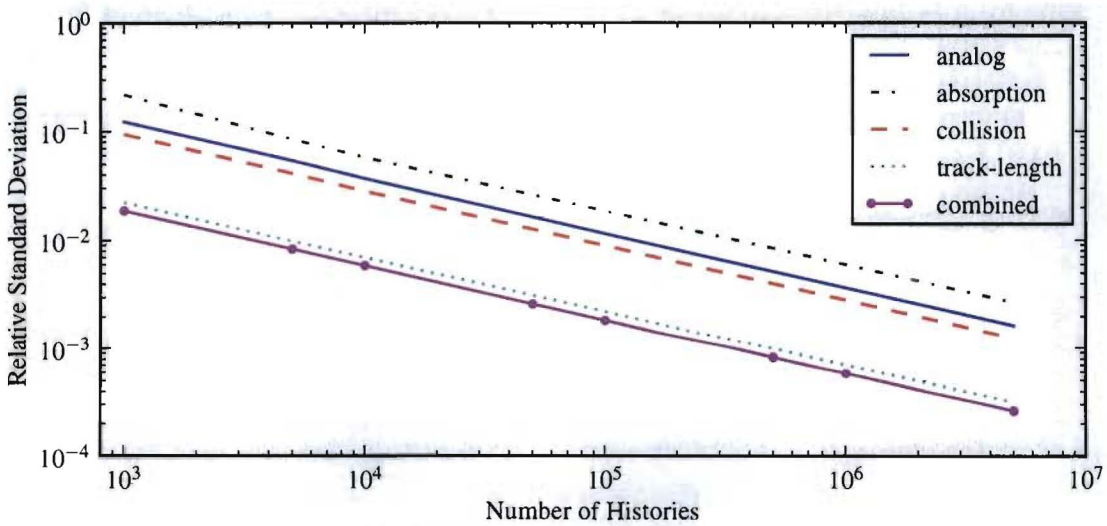

(b) Convergence rates of each estimator.

Figure 1: Momentum deposition estimates in one cell of an incident intensity problem with $\epsilon = ½$.

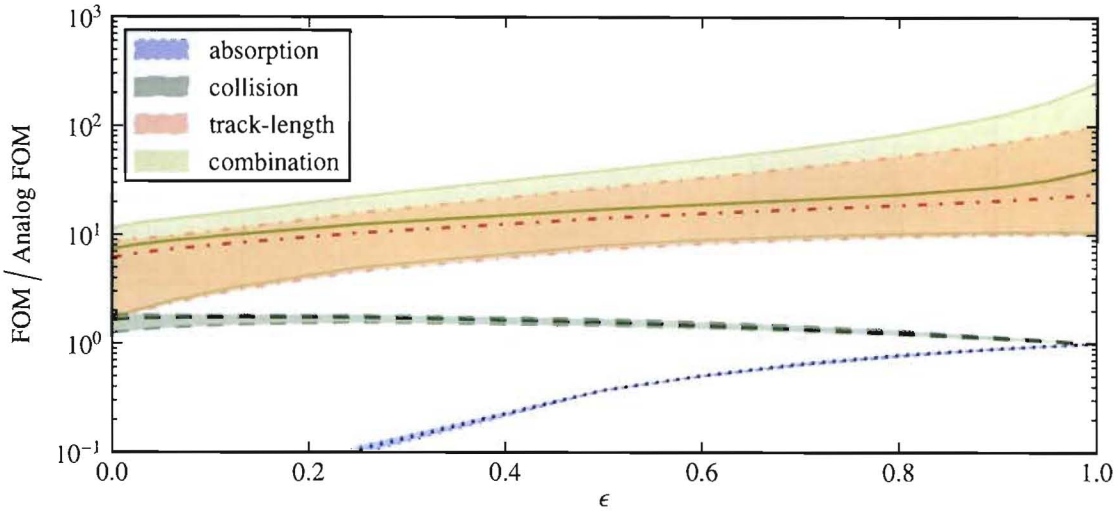

Figure 2: Incident intensity, analog-absorption tracking.

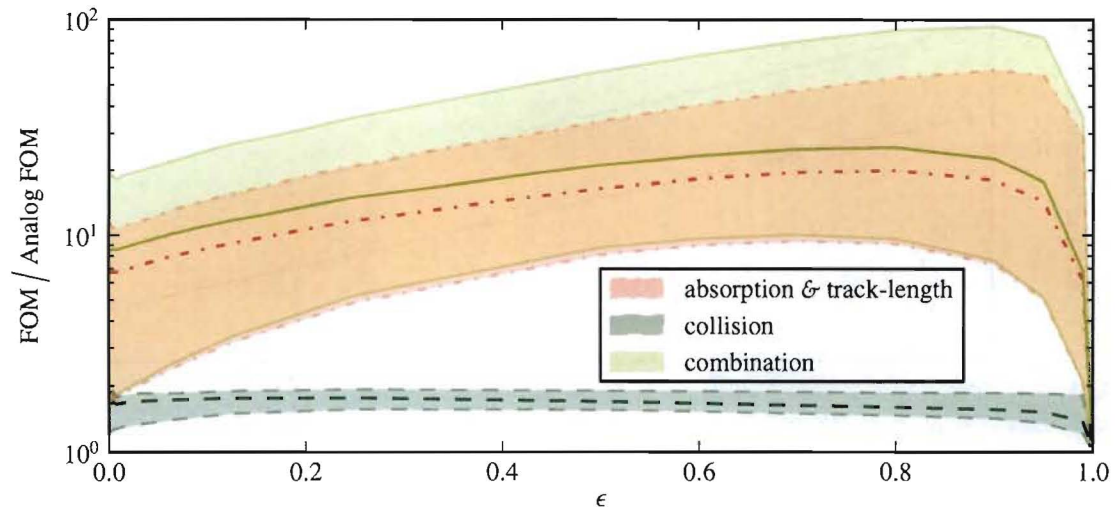

Figure 3: Incident intensity, implicit-absorption tracking.

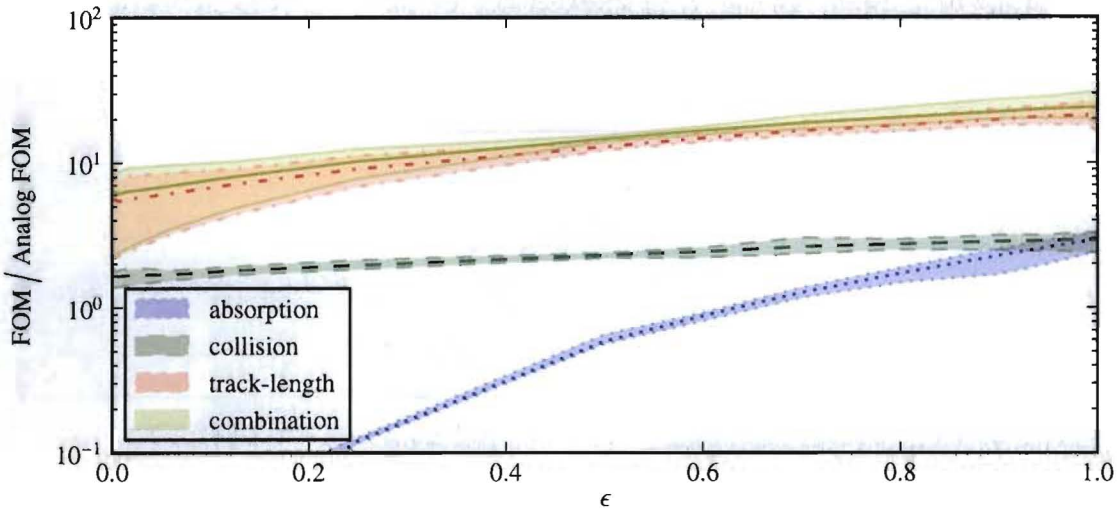

Figure 4: Radiation source, analog-absorption tracking.

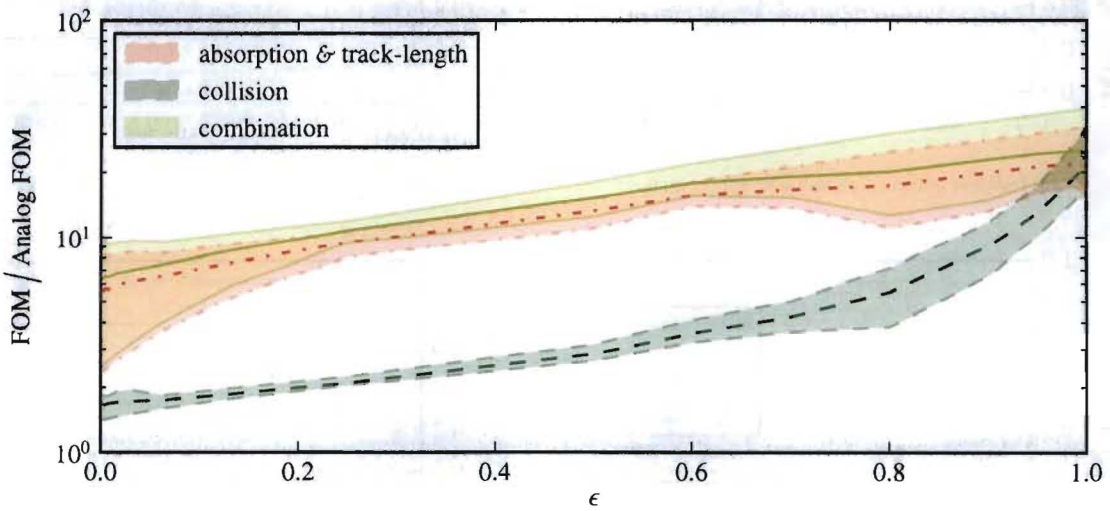

Figure 5: Radiation source, implicit-absorption tracking.

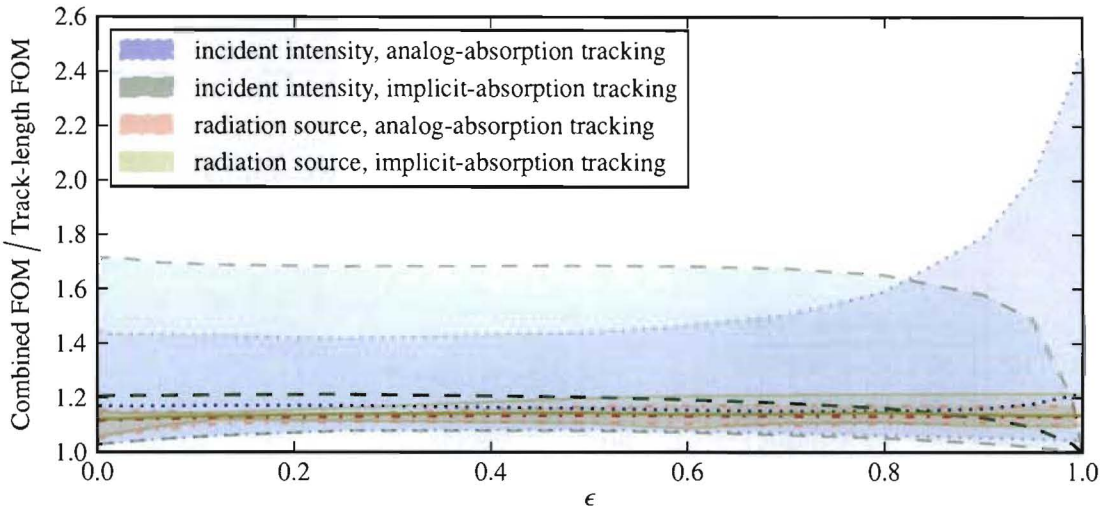

Figure 6: Comparison between combined and track-length estimator.

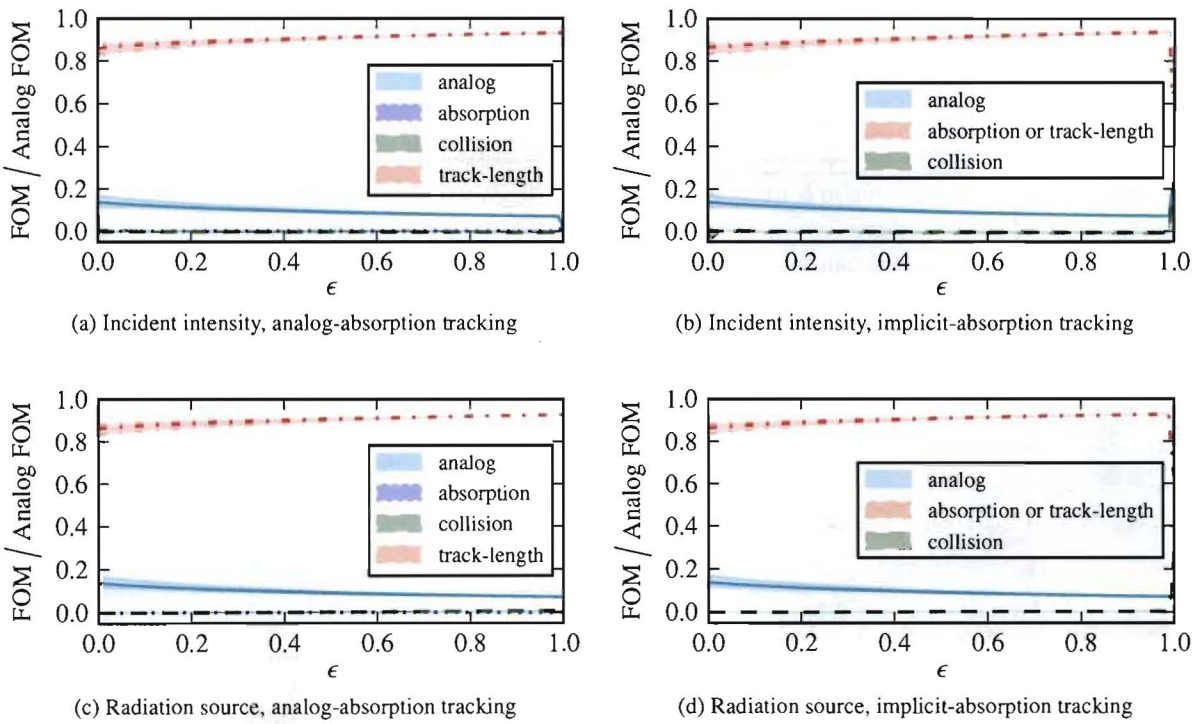

(a) Incident intensity, analog-absorption tracking

(b) Incident intensity, implicit-absorption tracking

(c) Radiation source, analog-absorption tracking

(d) Radiation source, implicit-absorption tracking

Figure 7: The weights used to compute the combined estimator.

5. CONCLUSIONS

After stating four Monte Carlo momentum deposition estimators and the equations for the mean and variance of a combined estimator, we have shown the benefits of the combined estimator quantitatively using the FOM. Over the range of problem and material types examined, the combined estimator FOM is greater than or equal to the track-length estimator FOM, the best solo estimator. In almost all cases, the combined estimator is at least a few percent better than the track-length estimator. The average FOM increase is in the 10–20% range, while the best gain was a factor of 1.7–2.5 better than the track-length estimator. The track-length estimator was the biggest term in the combined estimator sum, but the analog estimator also proved to be useful in the combination. The weights for the absorption and collision estimators were practically zero, implying that one would lose little by excluding them. Finally, in the numerical implementation, the truncated SVD method was robust in combining estimates that may be correlated.

ACKNOWLEDGEMENTS

This work was begun under U.S. government contract DE–AC52–06NA25396 for Los Alamos National Laboratory, which is operated by Los Alamos National Security, LLC, for the U.S. Department of Energy (DOE). The balance of the work was supported by the DOE Computational Science Graduate Fellowship of the first author, provided under grant DE–FG02–97ER25308. The authors wish to thank Jeffery Densmore and Yousry Azmy for helpful review of the manuscript.

REFERENCES

[1] Max Halperin, *Almost linearly-optimum combination of unbiased estimates*, Journal of the American Statistical Association **56** (1961), no. 293, 36–43.

[2] Joshua M. Hykes and Jeffrey D. Densmore, *Non-analog Monte Carlo estimators for radiation momentum deposition*, Journal of Quantitative Spectroscopy and Radiative Transfer **110** (2009), no. 13, 1097–1110.

[3] Edward W. Larsen, *Diffusion theory as an asymptotic limit of transport theory for nearly critical systems with small mean free paths*, Annals of Nuclear Energy **7** (1980), 249–255.

[4] Elmer E. Lewis and Warren F. Miller Jr, *Computational methods of neutron transport*, American Nuclear Society, La Grange Park, IL, 1993.

[5] The MathWorks, Inc., Natick, MA, *Matlab*, r2010a ed.

[6] Carl D. Meyer, *Matrix analysis and applied linear algebra*, Society for Industrial Mathematics, Philadelphia, 2000.

[7] Todd J. Urbatsch and Thomas M. Evans, *Milagro version 2, an implicit Monte Carlo code for thermal radiative transfer: capabilities, development, and usage*, Tech. Report LA-14195-MS, Los Alamos National Laboratory, 2006.

[8] Todd J. Urbatsch, R. Arthur Forster, Richard E. Prael, and Richard J. Beckman, *Estimation and Interpretation of k_{eff} Confidence Intervals in MCNP*, Tech. Report LA-12658, Los Alamos National Laboratory, 1995.

[9] _____, *Estimation and Interpretation of k_{eff} Confidence Intervals in MCNP*, Nuclear Technology **111** (1995), 169–182.